Physics Letters B 690 (2010) 466–472

Contents lists available at ScienceDirect

Physics Letters B

www.elsevier.com/locate/physletb

The spin-dependent structure function of the proton g_1^p and a test of the Bjorken sum rule

COMPASS Collaboration

M.G. Alekseev [ab], V.Yu. Alexakhin [g], Yu. Alexandrov [o], G.D. Alexeev [g], A. Amoroso [aa], A. Austregesilo [j,q], B. Badełek [ad], F. Balestra [aa], J. Ball [v], J. Barth [d], G. Baum [a], Y. Bedfer [v], J. Bernhard [m], R. Bertini [aa], M. Bettinelli [p], R. Birsa [x], J. Bisplinghoff [c], P. Bordalo [l,2], F. Bradamante [y], A. Bravar [x], A. Bressan [y], G. Brona [j,ad], E. Burtin [v], M.P. Bussa [aa], D. Chaberny [m], D. Čotić [m], M. Chiosso [aa], S.U. Chung [q], A. Cicuttin [x,z], M. Colantoni [ab], M.L. Crespo [x,z], S.Dalla Torre [x], S. Das [f], S.S. Dasgupta [f], O.Yu. Denisov [j,ab], L. Dhara [f], V. Diaz [x,z], S.V. Donskov [u], N. Doshita [b,af], V. Duic [y], W. Dünnweber [p], A. Efremov [g], A. El Alaoui [v], P.D. Eversheim [c], W. Eyrich [h], M. Faessler [p], A. Ferrero [aa,j], A. Filin [u], M. Finger [s], M. Finger jr. [g], H. Fischer [i], C. Franco [l], J.M. Friedrich [q], R. Garfagnini [aa], F. Gautheron [b], O.P. Gavrichtchouk [g], R. Gazda [ad], S. Gerassimov [o,q], R. Geyer [p], M. Giorgi [y], I. Gnesi [aa], B. Gobbo [x], S. Goertz [b,d], S. Grabmüller [q], A. Grasso [aa], B. Grube [q], R. Gushterski [g], A. Guskov [g], F. Haas [q], D. von Harrach [m], T. Hasegawa [n], F.H. Heinsius [i], R. Hermann [m], F. Herrmann [i], C. Heß [b], F. Hinterberger [c], N. Horikawa [r,3], Ch. Höppner [q], N. d'Hose [v], C. Ilgner [j,p], S. Ishimoto [r,4], O. Ivanov [g], Yu. Ivanshin [g], T. Iwata [af], R. Jahn [c], P. Jasinski [m], G. Jegou [v], R. Joosten [c], E. Kabuß [m], W. Käfer [i], D. Kang [i], B. Ketzer [q], G.V. Khaustov [u], Yu.A. Khokhlov [u], Yu. Kisselev [b], F. Klein [d], K. Klimaszewski [ad], S. Koblitz [m], J.H. Koivuniemi [b], V.N. Kolosov [u], K. Kondo [b,af], K. Königsmann [i], R. Konopka [q], I. Konorov [o,q], V.F. Konstantinov [u], A. Korzenev [m,5], A.M. Kotzinian [g,v], O. Kouznetsov [g,v], K. Kowalik [ad,v], M. Krämer [q], A. Kral [t], Z.V. Kroumchtein [g], R. Kuhn [q], F. Kunne [v], K. Kurek [ad], L. Lauser [i], J.M. Le Goff [v], A.A. Lednev [u], A. Lehmann [h], S. Levorato [y], J. Lichtenstadt [w], T. Liska [t], A. Maggiora [ab], M. Maggiora [aa], A. Magnon [v], G.K. Mallot [j,*], A. Mann [q], C. Marchand [v], J. Marroncle [v], A. Martin [y], J. Marzec [ae], F. Massmann [c], T. Matsuda [n], W. Meyer [b], T. Michigami [af], Yu.V. Mikhailov [u], M.A. Moinester [w], A. Mutter [i,m], A. Nagaytsev [g], T. Nagel [q], J. Nassalski [ad,1], T. Negrini [c], F. Nerling [i], S. Neubert [q], D. Neyret [v], V.I. Nikolaenko [u], A.S. Nunes [l], A.G. Olshevsky [g], M. Ostrick [m], A. Padee [ae], R. Panknin [d], D. Panzieri [ac], B. Parsamyan [aa], S. Paul [q], B. Pawlukiewicz-Kaminska [ad], E. Perevalova [g], G. Pesaro [y], D.V. Peshekhonov [g], G. Piragino [aa], S. Platchkov [v], J. Pochodzalla [m], J. Polak [k,y], V.A. Polyakov [u], G. Pontecorvo [g], J. Pretz [d], C. Quintans [l], J.-F. Rajotte [p], S. Ramos [l,2], V. Rapatsky [g], G. Reicherz [b], A. Richter [h], F. Robinet [v], E. Rocco [aa], E. Rondio [ad], D.I. Ryabchikov [u], V.D. Samoylenko [u], A. Sandacz [ad], H. Santos [l], M.G. Sapozhnikov [g], S. Sarkar [f], I.A. Savin [g], G. Sbrizzai [y], P. Schiavon [y], C. Schill [i], T. Schlüter [p], L. Schmitt [q,6], S. Schopferer [i], W. Schröder [h], O.Yu. Shevchenko [g], H.-W. Siebert [m], L. Silva [l], L. Sinha [f], A.N. Sissakian [g], M. Slunecka [g], G.I. Smirnov [g], S. Sosio [aa], F. Sozzi [y], A. Srnka [e], M. Stolarski [j], M. Sulc [k], R. Sulej [ae], S. Takekawa [y], S. Tessaro [x], F. Tessarotto [x], A. Teufel [h], L.G. Tkatchev [g], S. Uhl [q], I. Uman [p], M. Virius [t], N.V. Vlassov [g], A. Vossen [i], Q. Weitzel [q], R. Windmolders [d], W. Wiślicki [ad], H. Wollny [i], K. Zaremba [ae], M. Zavertyaev [o], E. Zemlyanichkina [g], M. Ziembicki [ae], J. Zhao [m,x], N. Zhuravlev [g], A. Zvyagin [p]

[a] *Universität Bielefeld, Fakultät für Physik, 33501 Bielefeld, Germany* [7]
[b] *Universität Bochum, Institut für Experimentalphysik, 44780 Bochum, Germany* [7]
[c] *Universität Bonn, Helmholtz-Institut für Strahlen- und Kernphysik, 53115 Bonn, Germany* [7]
[d] *Universität Bonn, Physikalisches Institut, 53115 Bonn, Germany* [7]
[e] *Institute of Scientific Instruments, AS CR, 61264 Brno, Czech Republic* [8]
[f] *Matrivani Institute of Experimental Research & Education, Calcutta-700 030, India* [9]

doi:10.1016/j.physletb.2010.05.069

[g] Joint Institute for Nuclear Research, 141980 Dubna, Moscow region, Russia
[h] Universität Erlangen–Nürnberg, Physikalisches Institut, 91054 Erlangen, Germany [7]
[i] Universität Freiburg, Physikalisches Institut, 79104 Freiburg, Germany [7]
[j] CERN, 1211 Geneva 23, Switzerland
[k] Technical University in Liberec, 46117 Liberec, Czech Republic [8]
[l] LIP, 1000-149 Lisbon, Portugal [10]
[m] Universität Mainz, Institut für Kernphysik, 55099 Mainz, Germany [7]
[n] University of Miyazaki, Miyazaki 889-2192, Japan [11]
[o] Lebedev Physical Institute, 119991 Moscow, Russia
[p] Ludwig-Maximilians-Universität München, Department für Physik, 80799 Munich, Germany [7,12]
[q] Technische Universität München, Physik Department, 85748 Garching, Germany [7,12]
[r] Nagoya University, 464 Nagoya, Japan [11]
[s] Charles University in Prague, Faculty of Mathematics and Physics, 18000 Prague, Czech Republic [8]
[t] Czech Technical University in Prague, 16636 Prague, Czech Republic [8]
[u] State Research Center of the Russian Federation, Institute for High Energy Physics, 142281 Protvino, Russia [13]
[v] CEA Irfu/SPhN Saclay, 91191 Gif-sur-Yvette, France
[w] Tel Aviv University, School of Physics and Astronomy, 69978 Tel Aviv, Israel [14]
[x] Trieste Section of INFN, 34127 Trieste, Italy
[y] University of Trieste, Department of Physics and Trieste Section of INFN, 34127 Trieste, Italy
[z] Abdus Salam ICTP and Trieste Section of INFN, 34127 Trieste, Italy
[aa] University of Turin, Department of Physics and Torino Section of INFN, 10125 Turin, Italy
[ab] Torino Section of INFN, 10125 Turin, Italy
[ac] University of Eastern Piedmont, 1500 Alessandria, and Torino Section of INFN, 10125 Turin, Italy
[ad] Sołtan Institute for Nuclear Studies and University of Warsaw, 00-681 Warsaw, Poland [15]
[ae] Warsaw University of Technology, Institute of Radioelectronics, 00-665 Warsaw, Poland [16]
[af] Yamagata University, Yamagata, 992-8510 Japan [11]

A R T I C L E I N F O

Article history:
Received 26 January 2010
Accepted 26 May 2010
Available online 1 June 2010
Editor: M. Doser

Keywords:
COMPASS
Deep inelastic scattering
Spin
Structure function
QCD analysis
Bjorken sum rule

A B S T R A C T

The inclusive double-spin asymmetry, A_1^p, has been measured at COMPASS in deep-inelastic polarised muon scattering off a large polarised NH_3 target. The data, collected in the year 2007, cover the range $Q^2 > 1$ $(\mathrm{GeV}/c)^2$, $0.004 < x < 0.7$ and improve the statistical precision of $g_1^p(x)$ by a factor of two in the region $x < 0.02$. The new proton asymmetries are combined with those previously published for the deuteron to extract the non-singlet spin-dependent structure function $g_1^{NS}(x, Q^2)$. The isovector quark density, $\Delta q_3(x, Q^2)$, is evaluated from a NLO QCD fit of g_1^{NS}. The first moment of Δq_3 is in good agreement with the value predicted by the Bjorken sum rule and corresponds to a ratio of the axial and vector coupling constants $|g_A/g_V| = 1.28 \pm 0.07$ (stat.) ± 0.10 (syst.).

In this Letter we present new COMPASS results for the longitudinal virtual photon–proton asymmetry, A_1^p, and for the spin structure function, g_1^p, in the deep inelastic scattering (DIS) region, covering the range 1 to 100 $(\mathrm{GeV}/c)^2$ in the photon virtuality Q^2 and 0.004 to 0.7 in the Bjorken scaling variable x.

In previous publications the COMPASS Collaboration has presented new accurate values of the longitudinal virtual photon–deuteron asymmetry, measured in the same kinematic range [1,2]. These new values have led to an improved determination of the spin structure function $g_1^d(x, Q^2)$ in the low x region where only the SMC measurements existed before [3]. The first moment of $g_1^d(x)$ has also provided a more accurate value for the matrix element of the flavour singlet axial current $a_0 = 0.35 \pm 0.03$ (stat.) $\pm$ 0.05 (syst.) at $Q^2 = 3$ $(\mathrm{GeV}/c)^2$, confirming the rather small contribution of the quark spins to the nucleon spin. In combination with the deuteron data, the new results on the proton yield an evaluation of the isovector non-singlet quark density, $\Delta q_3(x, Q^2) = (\Delta u + \Delta\bar{u})(x, Q^2) - (\Delta d + \Delta\bar{d})(x, Q^2)$, and its first moment which in turn provides a test of the Bjorken sum rule.

The proton data were collected in 2007 using a three target cell configuration and the upgraded COMPASS spectrometer, as described in [4]. The polarised target material is the ammonia previously used in the SMC experiment [5]. The polarisation was 0.9 in absolute value, measured with a relative error of 2% [6] for both polarisation signs. The muon beam has a natural polarisation of about −80%. The energy of the incoming muons is constrained to be in the interval $140 < E_\mu < 180$ GeV and their polarisation is known with a relative precision of ±5%. All events used in the present analysis are required to have a reconstructed primary in-

* Corresponding author.
E-mail address: gerhard.mallot@cern.ch (G.K. Mallot).
[1] Deceased.
[2] Also at IST, Universidade Técnica de Lisboa, Lisbon, Portugal.
[3] Also at Chubu University, Kasugai, Aichi, 487-8501 Japan.
[4] Also at KEK, 1-1 Oho, Tsukuba, Ibaraki, 305-0801 Japan.
[5] On leave of absence from JINR Dubna.
[6] Also at GSI mbH, Planckstr. 1, D-64291 Darmstadt, Germany.
[7] Supported by the German Bundesministerium für Bildung und Forschung.
[8] Supported by Czech Republic MEYS grants ME492 and LA242.
[9] Supported by SAIL (CSR), Govt. of India.
[10] Supported by the Portuguese FCT – Fundação para a Ciência e Tecnologia grants POCTI/FNU/49501/2002 and POCTI/FNU/50192/2003.
[11] Supported by the MEXT and the JSPS under Grants Nos. 18002006, 20540299 and 18540281; Daiko Foundation and Yamada Foundation.
[12] Supported by the DFG cluster of excellence 'Origin and Structure of the Universe' (http://www.universe-cluster.de).
[13] Supported by CERN-RFBR grant 08-02-91009.
[14] Supported by the Israel Science Foundation, founded by the Israel Academy of Sciences and Humanities.
[15] Supported by Ministry of Science and Higher Education grant 41/N-CERN/2007/0.
[16] Supported by KBN grant Nr. 134/E-365/SPUB-M/CERN/P-03/DZ299/2000.

teraction vertex (defined by the incoming and the scattered muon) inside one of the target cells. In order to cancel out the muon flux normalisation in the asymmetry calculation, incident muons are only accepted when their extrapolated trajectory crosses all three cells. The reconstruction procedure is described in Ref. [7].

Events are triggered using three different sets of conditions. Inclusive triggers, which cover the full range of x, are based on combinations of hodoscope signals defining the trajectory of the scattered muon. Semi-inclusive triggers, which cover mainly the region $x < 0.1$, require a condition on the energy deposit in the hadron calorimeter in addition to the hodoscope signals. Calorimeter-only triggers, without any input from hodoscopes, cover the large x and Q^2 regions. For the calorimeter triggers, as well as for the semi-inclusive ones, the presence of a reconstructed hadron trajectory compatible with the calorimeter information is required.

The kinematic region is defined by requiring the photon virtuality $Q^2 > 1\ (\mathrm{GeV}/c)^2$ and the fractional energy y transfered from the beam muon to the virtual photon to be between 0.1 and 0.9. The region which is most affected by QED radiative corrections is eliminated by the cut $y < 0.9$. The total sample after all cuts amounts to 85.3 million events.

The longitudinal virtual-photon–proton asymmetry, A_1^p, is evaluated from the numbers of events collected in the different target cells by the method used in our previous analyses of deuteron data [1,2]. Neighbouring target cells are polarised in opposite directions and data from both target spin orientations are thus recorded simultaneously. Since the transverse asymmetry contribution is negligible at the COMPASS energy the relation between A_1^p and the counting rate asymmetry A^{exp} reduces to

$$A_1^p = \frac{1}{P_B P_T D f} A^{\mathrm{exp}} \tag{1}$$

where P_B and P_T are the beam and target polarisations, D the depolarisation factor of the virtual photon and f the target dilution factor. The lengths of the cells are chosen so that the two samples collected with opposite spin orientations have in average the same acceptance, which limits the possible biases due to false asymmetry contributions. The target spin directions are reversed once per day by rotating the magnetic field and a few times per year by changing the microwave frequencies used for dynamic nuclear polarisation. The asymmetries are calculated from the numbers of events in cells with opposite spin orientations collected before and after a field rotation so that flux and acceptance factors cancel out. In order to minimise the statistical error, all quantities used in the asymmetry calculation are evaluated event by event with the weight factor

$$w = P_B f D. \tag{2}$$

The polarisation of the beam muon, P_B, is obtained from a parameterisation as a function of the beam momentum. The factors f and D are calculated from the kinematic variables.

Radiative corrections are applied separately to the asymmetries obtained for the inclusive triggers and to those obtained for the semi-inclusive and calorimeter-only triggers because radiative elastic events contribute only to the former ones. Another correction is applied to account for the polarisation of the ^{14}N nucleus. For this spin 1 object the correction is proportional to A_1^d which can be parametrised as a function of x only, and affected by factors accounting for the number of ^{14}N nuclei vs. ^{1}H atoms, the alignment of the proton spin vs. the ^{14}N spin and the ratio of ^{14}N to ^{1}H polarisations [8]:

$$\Delta A_1^p(x) = \frac{1}{3} \cdot \left(-\frac{1}{3}\right) \cdot \frac{1}{6} \cdot \frac{\sigma_d(x)}{\sigma_p(x)} \cdot A_1^d(x). \tag{3}$$

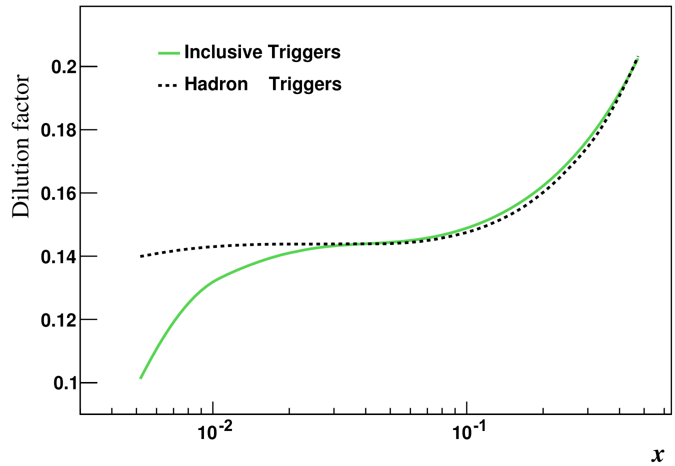

Fig. 1. The dilution factor f of the NH_3 polarised target as a function of x for inclusive and for semi-inclusive hadron triggers [3]. The values of $f(x)$ are averaged over the Q^2 range of the corresponding triggers.

The corrections for the various intervals of x are given in Table 5. They are of the order of 0.01 for $x > 0.35$ and increase the value of the first moment of the spin structure function $\Gamma_1^p(Q^2) = \int_0^1 g_1^p(x, Q^2)\,dx$ by about 1%.

The target dilution factor f is given by the ratio of the cross-section for the polarisable protons to that of all nuclei in a target cell. The values for the NH_3 target are shown in Fig. 1 as a function of x, for inclusive and hadron triggers. They are about 14% in the medium x region, with a rise at large x due to the reduced cross section on heavy targets in this region, and a drop at low x for inclusive triggers due to the contribution of radiative elastic events on the proton.

The new values of $A_1^p(x)$ are shown in Fig. 2 in comparison with results from previous experiments. The Q^2 of different points at any fixed value of x varies considerably since the incident energy of the various experiments ranges from 6 to 200 GeV. The fact that all results align reasonably well on a single curve illustrates the well known observation that the Q^2 dependence of A_1^p is very weak in the DIS region. This is further illustrated in Fig. 3 which shows A_1^p as a function of Q^2 in intervals of x for the COMPASS data. No significant Q^2 dependence is observed in any interval of x.

The systematic errors of the COMPASS results for A_1^p are shown by the band at the bottom of Fig. 2 and listed in Table 1. They contain the contributions due to the uncertainties on the beam polarisation, the target polarisation, the ratio $R = \sigma_L/\sigma_T$ [9] used in the depolarisation factor and the dilution factor, which are equal to 5, 2, at most 3 and 1%, respectively. Combined in quadrature, these uncertainties amount to a correlated systematic error of at most 6% of the quoted value. The error due to the neglect of the transverse asymmetry, A_2^p, multiplied by a kinematic factor η, is less than 0.002 in the full range of x and the error due to the QED radiative corrections less than 0.001. Another possible contribution to the systematic error is due to false asymmetries generated by instabilities in some components of the spectrometer. Such effects have been searched for in faked configurations, where the physics asymmetry does not contribute, and were found to be compatible with zero. The comparison of results obtained with opposite orientations of the target field also does not show any significant difference. The possible error due to false asymmetries has been estimated by a statistical test performed on the distribution of asymmetries extracted from 46 subsamples. Time-dependent effects which would lead to a broadening of these distributions were

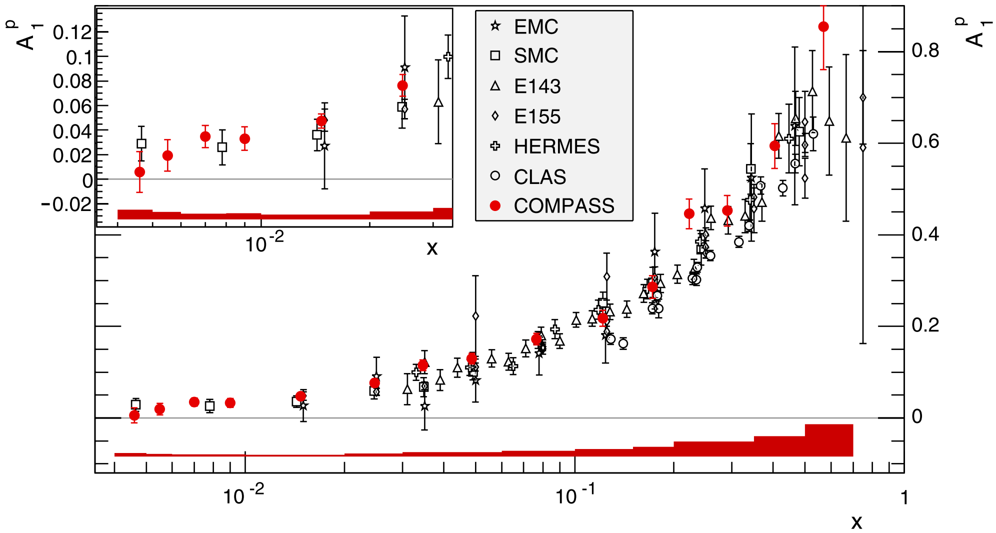

Fig. 2. The asymmetry $A_1^p(x)$ as measured by COMPASS and previous results from EMC [10], SMC [3], HERMES [11], SLAC E143 [12], E155 [13] and CLAS [14] at $Q^2 > 1\ (\mathrm{GeV}/c)^2$. The cut $W > 2.5$ GeV has been applied to select DIS events in the CLAS data. Only statistical errors are shown with the data points. The band at the bottom shows the systematic errors for the COMPASS data.

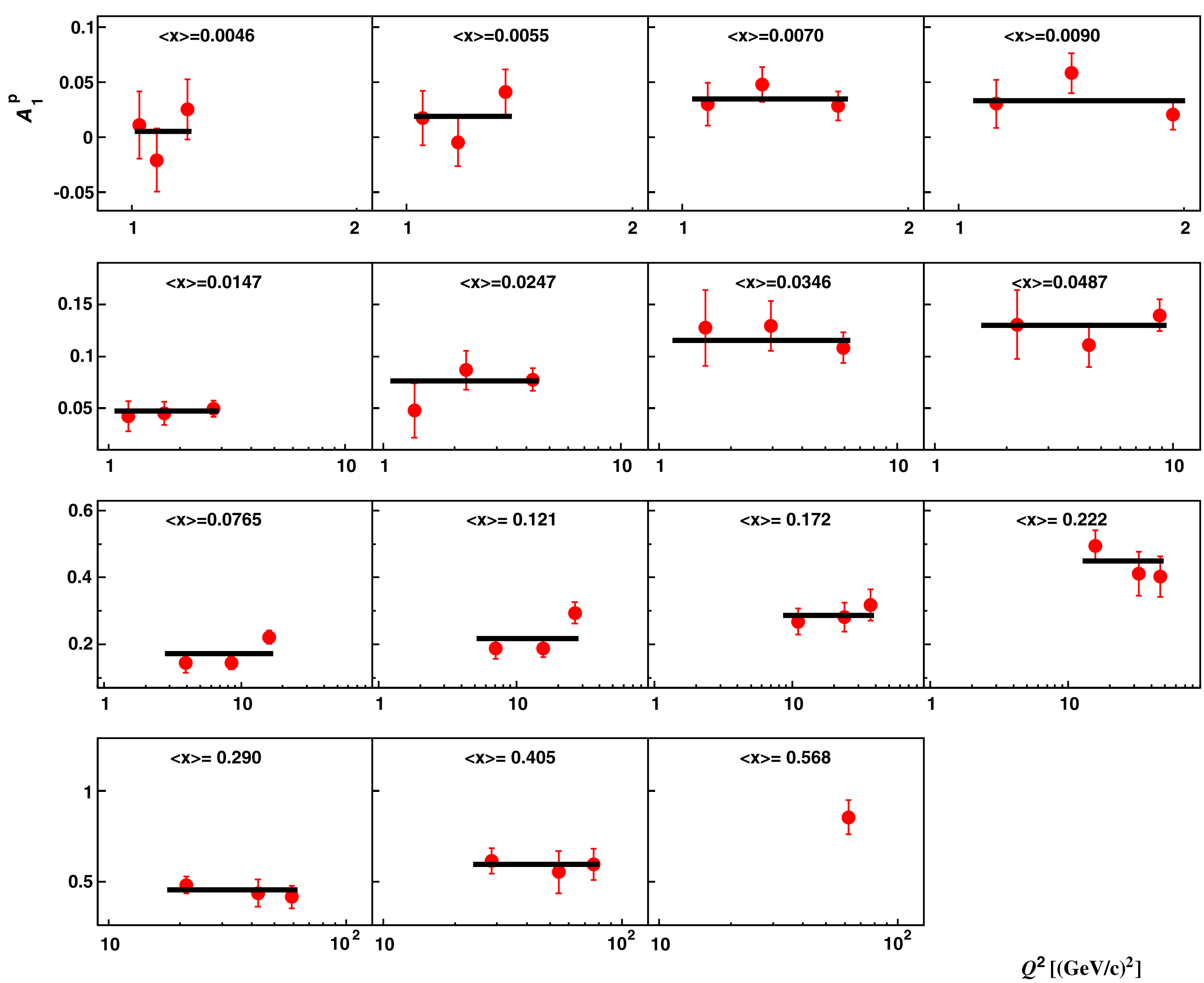

Fig. 3. Values of $A_1^p(x, Q^2)$ as a function of Q^2 for each interval of x. The errors are statistical only. The lines show the average values quoted in Table 1.

Table 1
Values of A_1^p and g_1^p as a function of x with the corresponding average value of Q^2. The first error is statistical, the second one systematical.

x range	$\langle x \rangle$	$\langle Q^2 \rangle$ [(GeV/c)^2]	A_1^p	g_1^p
0.004–0.005	0.0046	1.10	$0.006 \pm 0.017 \pm 0.008$	$0.133 \pm 0.389 \pm 0.183$
0.005–0.006	0.0055	1.20	$0.019 \pm 0.013 \pm 0.006$	$0.385 \pm 0.256 \pm 0.123$
0.006–0.008	0.0070	1.37	$0.035 \pm 0.009 \pm 0.005$	$0.571 \pm 0.147 \pm 0.079$
0.008–0.010	0.0090	1.59	$0.033 \pm 0.010 \pm 0.005$	$0.445 \pm 0.130 \pm 0.067$
0.010–0.020	0.0147	2.14	$0.047 \pm 0.006 \pm 0.004$	$0.427 \pm 0.052 \pm 0.036$
0.020–0.030	0.0247	3.24	$0.076 \pm 0.009 \pm 0.006$	$0.459 \pm 0.053 \pm 0.037$
0.030–0.040	0.0346	4.36	$0.115 \pm 0.012 \pm 0.009$	$0.525 \pm 0.054 \pm 0.041$
0.040–0.060	0.0487	6.05	$0.130 \pm 0.012 \pm 0.010$	$0.438 \pm 0.039 \pm 0.032$
0.060–0.100	0.0765	9.42	$0.172 \pm 0.013 \pm 0.012$	$0.383 \pm 0.028 \pm 0.026$
0.100–0.150	0.122	14.9	$0.218 \pm 0.017 \pm 0.015$	$0.303 \pm 0.024 \pm 0.021$
0.150–0.200	0.172	20.9	$0.286 \pm 0.024 \pm 0.020$	$0.268 \pm 0.023 \pm 0.019$
0.200–0.250	0.222	26.7	$0.446 \pm 0.032 \pm 0.030$	$0.298 \pm 0.022 \pm 0.020$
0.250–0.350	0.290	34.6	$0.453 \pm 0.033 \pm 0.032$	$0.196 \pm 0.014 \pm 0.013$
0.350–0.500	0.405	47.1	$0.594 \pm 0.049 \pm 0.043$	$0.120 \pm 0.010 \pm 0.008$
0.500–0.700	0.568	62.1	$0.855 \pm 0.094 \pm 0.068$	$0.048 \pm 0.005 \pm 0.004$

Table 2
Decomposition of the systematic error of A_1^p into multiplicative (top) and additive (bottom) contributions.

Beam polarisation	$\Delta P_b/P_b$	$0.04/0.8 = 5.0\%$
Target polarisation	$\Delta P_t/P_t$	2%
Depolarisation factor	$\Delta D(R)/D(R)$	2.0–3.0%
Dilution factor	$\Delta f/f$	1%
Total	ΔA_1^{mult}	$\simeq 0.06 A_1$
Transverse asymmetry	$\eta \cdot A_2$	$< 2.0 \times 10^{-3}$
Rad. corrections	ΔA_1^{RC}	10^{-4}–10^{-3}
False asymmetry	A_{false}	$< 0.47 \cdot \Delta A_1^{stat}$

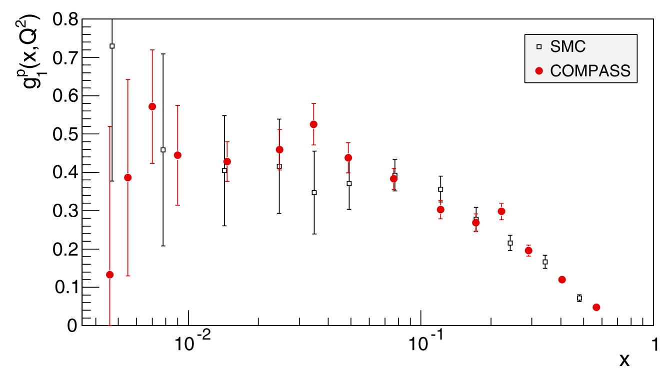

Fig. 4. The spin structure function $g_1^p(x, Q^2)$ vs. x as measured by COMPASS at the Q^2 of each measured point. Previous results from SMC [3] are shown for comparison. The errors are statistical only.

not observed. As a consequence the limit $\sigma_{syst} < 0.47\sigma_{stat}$ was obtained at the level of one standard deviation. The different contributions to the systematic error are summarised in Table 2.

The longitudinal spin structure function g_1^p of the proton is obtained from A_1^p by the relation

$$g_1^p = \frac{F_2^p}{2x(1+R)} A_1^p \tag{4}$$

where F_2^p is the spin-independent structure function. The values obtained with the SMC parameterisation of the world data on F_2^p [3] and the parameterisation of R already used in the depolarisation factor are listed in Table 1 with their statistical and systematic errors. They are also shown in Fig. 4 in comparison with the SMC values. It can be seen that the COMPASS data improve the statistical precision at least by a factor of two in the low x region, covered only by the two experiments shown here. The new data points are compatible with a constant $g_1^p(x)$ for $0.004 < x < 0.04$ and do not show evidence either for an increase or a decrease when x decreases towards the kinematic limit of 0.004. This observation remains valid when the data points are moved to a common Q^2 according to the fits quoted in Ref. [2] and the constant value is found to be $g_1^p = 0.48 \pm 0.03$ (stat.) ± 0.04 (syst.) at $Q^2 = 3$ (GeV/c)^2.

The non-singlet spin structure function

$$g_1^{NS}(x, Q^2) = g_1^p(x, Q^2) - g_1^n(x, Q^2) \tag{5}$$

is of special interest because its Q^2 dependence is decoupled from the singlet quark and the gluon spin densities:

$$g_1^{NS}(x, Q^2) = \frac{1}{6}\int_x^1 \frac{dx'}{x'} C^{NS}\left(\frac{x}{x'}, \alpha_s(Q^2)\right) \Delta q_3(x', Q^2) \tag{6}$$

where C^{NS} is a Wilson coefficient function and Δq_3 the isovector non-singlet spin density. Consequently a fit of the Q^2 evolution of g_1^{NS} requires only a small number of parameters to describe the shape of $\Delta q_3(x)$ at some reference Q^2.

In the present analysis, $Q_0^2 = 3$ (GeV/c)^2 is taken as reference Q^2 in the fit and the following parameterisation used for Δq_3:

$$\Delta q_3(x, Q_0^2) = \eta_3 \frac{x^{\alpha_3}(1-x)^{\beta_3}}{\int_0^1 x^{\alpha_3}(1-x)^{\beta_3}\, dx}. \tag{7}$$

The input values of g_1^{NS} are obtained as

$$g_1^{NS}(x, Q^2) = 2\left[g_1^p(x, Q^2) - \frac{g_1^d(x, Q^2)}{1 - 1.5\omega_D}\right] \tag{8}$$

where the values of g_1^d are taken from Ref. [2] and the deuteron D-state probability, ω_D, is 0.05 ± 0.01 [15]. The proton and deuteron data have been obtained at the same (x, Q^2) points, which avoids the need of interpolation. A correction has however to be applied to the deuteron data for the admixtures of ^{7}Li and ^{1}H in the ^{6}LiD target material, which was not taken into account in Ref. [2]. The ratios of isotopes ^{7}Li/^{6}Li and H/D were found to be 4.4% and 0.5% respectively [16] and ^{7}Li and ^{1}H are both polarised at more than 90% [17]. The resulting corrections to A_1^d are given in Table 5. They are negligible at low x but reach 0.015 at $x = 0.50$ and reduce the first moment Γ_1^d by 0.002.

The values of $\alpha_s(Q^2)$ used in the fit are evolved at next to leading order (NLO) from $\alpha(M_Z^2) = 0.1187$. Higher twist contributions to g_1^{NS} are not taken into account because most data points are at $Q^2 > 3$ (GeV/c)^2, a region where they are expected to be negligible [18,19]. As for our previous analysis [2] the QCD fit at NLO of the COMPASS values of g_1^{NS} to Eq. (6) has been performed with two different programs, the first one working in the (x, Q^2) space [20], the second one in the space of moments [21]. Both programs give the same values of the fitted parameters, listed in Table 3, and similar χ^2-probabilities. The fitted distribution of $xg_1^{NS}(x)$ and the data points moved to the reference Q^2 are shown in Fig. 5 (left). The Bjorken sum rule predicts that η_3, the first moment of Δq_3, should be equal to the value of the ratio $|g_A/g_V|$ of the axial and vector coupling constants derived from neutron β decay ($|g_A/g_V| = 1.2694 \pm 0.0028$ [22]). The two values are found to agree within one standard deviation. The sum rule is thus satisfied in a test free of systematic errors arising from uncertainties on the gluon helicity distribution. The χ^2-probability of the fit, also given in Table 3, shows that the data are in good agreement with the simple parameterisation of Eq. (7) and do not require a more flexible distribution. The exponent α_3 is in the range of Regge pole predictions [23].

The integral of g_1^{NS} at any fixed Q^2 is given by the relation

$$\Gamma_1^{NS}(Q^2) = \frac{1}{6}\left|\frac{g_A}{g_V}\right| C_1^{NS}(Q^2) \qquad (9)$$

where the non-singlet coefficient function $C_1^{NS}(Q^2)$ is known in perturbative QCD up to the third order in $\alpha_s(Q^2)$ [24]. As a cross-check we have evaluated the integral of g_1^{NS} at $Q^2 = 3\ (\mathrm{GeV}/c)^2$ directly from the data in the range $0.004 < x < 0.7$ with additional low and high x contributions taken from the fit (Table 4). It is observed that about 92% of the first moment Γ_1^{NS} comes from the measured region. The dependence of the first moment of g_1^{NS} on its lower limit is shown in Fig. 5 (right). As already observed in the HERMES analysis [11], the integral does not saturate at $x \approx 0.01$–0.02 while the value obtained at the lowest x accessible in the present analysis (0.180 ± 0.009) is less than one standard deviation below the value expected from the Bjorken sum rule (0.188). The value of $|g_A/g_V|$ derived from the value of Γ_1^{NS} by Eq. (9) is identical to the one obtained from the fit and confirms the validity of the Bjorken sum rule with a statistical precision of 5%.

The dominant systematic error on this result is due to the uncertainty of 5% on the beam polarisation, which is common to the proton and deuteron data and therefore translates directly into a 5% error on $|g_A/g_V|$. Other contributions due to the target polarisation and the dilution factor are estimated to be 0.04 and 0.06 for the proton and deuteron terms, respectively. The resulting systematic error is 0.10. The errors related to the fit or to the evolution of

Table 3
Results of the fits of $\Delta q_3(x)$ at $Q^2 = 3\ (\mathrm{GeV}/c)^2$.

Param.	Value
η_3	1.28 ± 0.07
α_3	-0.22 ± 0.07
β_3	$2.2\pm^{0.5}_{0.4}$
χ^2/ND	14.4/12
Prob.	0.27

Table 4
First moment Γ_1^{NS} at $Q^2 = 3\ (\mathrm{GeV}/c)^2$ from the COMPASS data points. The contributions from the unmeasured regions are estimated from the NLO fit to g_1^{NS}; their errors are negligible.

x range	Γ_1^{NS}
0–0.004	0.0098
0.004–0.7	$0.175 \pm 0.009 \pm 0.015$
0.7–1.0	0.0048
0–1	$0.190 \pm 0.009 \pm 0.015$

Table 5
Corrections to the COMPASS spin asymmetries A_1^p and A_1^d due to the ^{14}N polarisation and to the admixture of ^{7}Li and ^{1}H into the ^{6}LiD target material. In both cases the correction must be subtracted from the measured asymmetries. The corrections to A_1^p are already applied to the values quoted in the present Letter.

x range	Corr. to A_1^p	Corr. to A_1^d
0.004–0.005	0.000	0.000
0.005–0.006	0.000	0.000
0.006–0.008	0.000	0.001
0.008–0.010	0.000	0.001
0.010–0.020	0.000	0.001
0.020–0.030	0.000	0.001
0.030–0.040	−0.000	0.002
0.040–0.060	−0.001	0.002
0.060–0.100	−0.001	0.003
0.100–0.150	−0.003	0.004
0.150–0.200	−0.004	0.006
0.200–0.250	−0.005	0.008
0.250–0.350	−0.006	0.010
0.350–0.500	−0.009	0.013
0.500–0.700	−0.014	0.017

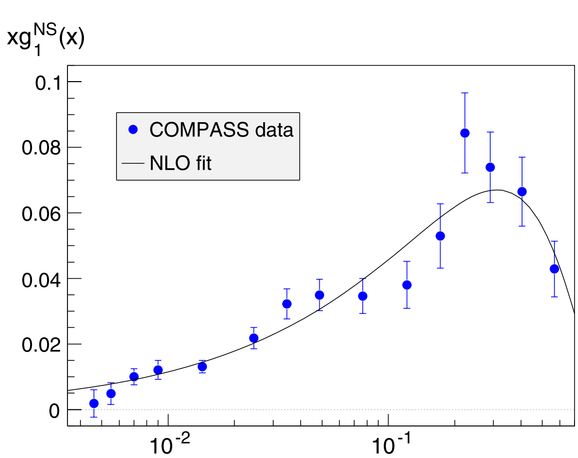

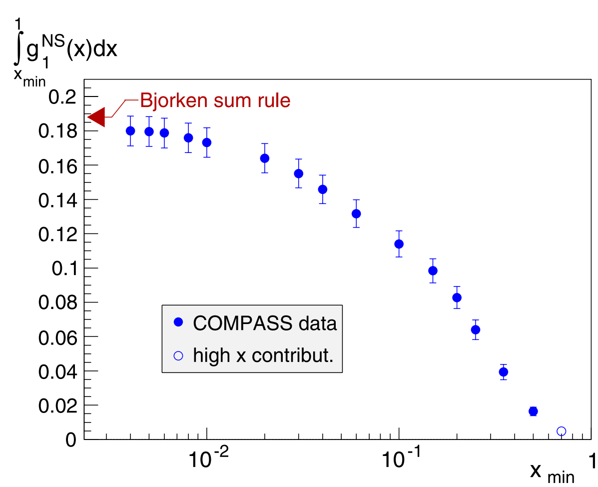

Fig. 5. Left: Values of $g_1^{NS}(x)$ at $Q^2 = 3\ (\mathrm{GeV}/c)^2$, derived from the COMPASS measurements of A_1^p and A_1^d and result of a three parameter QCD fit at NLO. The errors are statistical only. Right: $\int_{x_{\min}}^1 g_1^{NS}\,dx$ as a function of $x_{\min}$ as obtained from the COMPASS data points. The open circle at $x = 0.7$ is obtained from the fit. The arrow on the left side shows the value expected for the full range $0 < x < 1$ with $|g_A/g_V| = 1.269$ [22].

the data to a common Q^2 are found to be negligible. In particular, it was checked that the same value of g_A/g_V is obtained when the reference Q^2 is 1.0, 3.0 or 10.0 $(\text{GeV}/c)^2$ although the exponent α_3 varies from -0.15 to -0.28 when Q^2 is moved from 1 to 10 and the shape of $g_1^{NS}(x)$ thus becomes quite different.

The test of the Bjorken sum rule performed in the present analysis of the COMPASS proton and deuteron data is thus mainly limited by systematics:

$$\left|\frac{g_A}{g_V}\right| = 1.28 \pm 0.07\ (\text{stat.}) \pm 0.10\ (\text{syst.}), \tag{10}$$

to be compared with the value 1.2694 ± 0.0028 derived from neutron β decay [22].

The COMPASS value of Γ_1^{NS} at $Q^2 = 10\ (\text{GeV}/c)^2$ is $0.195 \pm 0.009 \pm 0.015$, in good agreement with the one obtained by the SMC at the same Q^2 ($0.198 \pm 0.016 \pm 0.014$) [3], and improves the statistical precision almost by a factor 2. The cumulative integral of g_1^{NS} truncated at $x_{\min} = 0.021$ is equal to 0.1583 ± 0.0085 (stat.) $\pm$ 0.014 (syst.), in good agreement with the HERMES value of 0.1484 ± 0.0055 (stat.) $\pm$ 0.0160 (syst.) obtained at $Q^2 = 5\ (\text{GeV}/c)^2$ [11].

In conclusion, the COMPASS Collaboration has performed new measurements of the longitudinal spin asymmetry of the proton, covering a large range of x ($0.004 < x < 0.7$) in the DIS region, $Q^2 > 1\ (\text{GeV}/c)^2$. The new data improve the statistical precision in the low x region by a factor of 2–3 and show no evidence either for an increase or a decrease of the spin structure function g_1^p in this region. In combination with the previously published results on the deuteron, the new data improve the evaluation of the non-singlet spin structure function g_1^{NS} and provide a test of the Bjorken sum rule, which is satisfied within one standard deviation of the statistical uncertainty.

Acknowledgements

We gratefully acknowledge the support of the CERN management and staff and the skill and effort of the technicians of our collaborating institutes. Special thanks go to V. Anosov and V. Pesaro for their technical support during the installation and the running of this experiment. This work was made possible thanks to the financial support of our funding agencies.

References

[1] COMPASS Collaboration, E.S. Ageev, et al., Phys. Lett. B 612 (2005) 154.
[2] COMPASS Collaboration, V.Yu. Alexakhin, et al., Phys. Lett. B 647 (2007) 8.
[3] SMC Collaboration, B. Adeva, et al., Phys. Rev. D 58 (1998) 112001.
[4] COMPASS Collaboration, M. Elusive, et al., Phys. Lett. B 680 (2009) 217.
[5] SMC Collaboration, B. Adeva, et al., Phys. Lett. B 412 (1997) 414.
[6] Yu. Kisselev, et al., Spin Interactions in Ammonia and Methods to Cross-check Polarisation, Spin Praha 08, Advanced Studies Institute, Symmetries and Spin, July 20–26, 2008.
[7] V. Aleksakhin, Y. Bedfer, S. Gerasimov, A. Korzenev, Phys. Part. Nucl. Lett. 4 (2007) 350.
[8] O.A. Rondon, Phys. Rev. C 60 (1999) 035201.
[9] E143 Collaboration, K. Abe, et al., Phys. Lett. B 452 (1999) 194.
[10] EMC Collaboration, J. Ashman, et al., Phys. Lett. B 206 (1988) 364;
EMC Collaboration, J. Ashman, et al., Nucl. Phys. B 328 (1989) 1.
[11] HERMES Collaboration, A. Airapetian, et al., Phys. Rev. D 75 (2007) 012007.
[12] E143 Collaboration, K. Abe, et al., Phys. Rev. D 58 (1998) 112003.
[13] E155 Collaboration, P.L. Anthony, et al., Phys. Lett. B 493 (2000) 19.
[14] CLAS Collaboration, K.V. Dharmawardane, et al., Phys. Lett. B 641 (2006) 11.
[15] R. Machleidt, K. Holinde, C. Elster, Phys. Rep. 149 (1987) 1.
[16] S. Neliba, et al., Nucl. Instrum. Meth. A 526 (2004) 144.
[17] J. Ball, et al., Nucl. Instrum. Meth. A 498 (2003) 101.
[18] E. Leader, A.V. Sidorov, D.B. Stamenov, Phys. Rev. D 75 (2007) 074027.
[19] R.S. Pasechnik, et al., Phys. Rev. D 81 (2010) 016010.
[20] SMC Collaboration, B. Adeva, et al., Phys. Rev. D 58 (1998) 112002.
[21] A.N. Sissakian, O.Yu. Shevchenko, O.N. Ivanov, Phys. Rev. D 70 (2004) 074032.
[22] Particle Data Group, C. Amsler, et al., Phys. Lett. B 667 (2008) 1.
[23] S.D. Bass, Mod. Phys. Lett. A 22 (2007) 1005.
[24] S.A. Larin, T. van Ritbergen, J.A.M. Vermaseren, Phys. Lett. B 404 (1997) 153.